MASSACHUSETTS INSTITUTE OF TECHNOLOGY
ARTIFICIAL INTELLIGENCE LABORATORY

and

CENTER FOR BIOLOGICAL INFORMATION PROCESSING
WHITAKER COLLEGE

A.I. Memo 786
C.B.I.P. Paper 010

November 1984

The Coordination of Arm Movements
An Experimentally Confirmed Mathematical Model

Tamar Flash and Neville Hogan

Abstract: This paper presents studies of the coordination of voluntary human arm movements. A mathematical model is formulated which is shown to predict both the qualitative features and the quantitative details observed experimentally in planar, multi-joint arm movements. Coordination is modelled mathematically by defining an objective function, a measure of performance for any possible movement. The unique trajectory which yields the best performance is determined using dynamic optimization theory. In the work presented here the objective function is the square of the magnitude of jerk (rate of change of acceleration) of the hand integrated over the entire movement. This is equivalent to assuming that a major goal of motor coordination is the production of the smoothest possible movement of the hand. The theoretical analysis is based solely on the kinematics of movement independent of the dynamics of the musculoskeletal system, and is successful only when formulated in terms of the motion of the hand in extracorporal space. The implications with respect to movement organization are discussed.

This report describes research done within the Artificial Intelligence Laboratory and the Center for Biological Information Processing (Whitaker College) at the Massachusetts Institute of Technology. Support for the A. I. Laboratory's research in artificial intelligence is provided in part by the Advanced Research Projects Agency of the Department of Defense under Office of Naval Research contract N00014-80-C-0505. The Center's support is provided in part by the Sloan Foundation and in part by the Whitaker College. Additional support was provided by the National Institute of Neurological Disease and Stroke Research Grant NS09343 and by the National Institute of Arthritis, Metabolism, and Digestive Diseases Grant AM26710. Tamar Flash was supported by the Whitaker Health Sciences Fund and by the Bantrell Fellowship. The authors wish to thank Drs. William Abend, Emilio Bizzi, Pierro Morasso and John Hollerbach for their insightful comments and for making their experimental data available to us.

Introduction

How is movement control organized? Which variable(s) are controlled? These questions have become a growing concern of motor neurophysiologists [Granit 1981, Stein 1982]. Although investigations have traditionally focused on single muscle contractions or single-joint movements, these systems cannot reveal the problems confronted by the central nervous system in the control of normal multi-joint movements. Even a two-joint motion is vastly more complicated than a single-joint motion; in moving from one point to another, on what basis does the central nervous system select one specific trajectory from the infinite number possible? In what coordinate frame is the trajectory planned? However, these complexities offer new research opportunities; investigations of multi-joint movements may provide considerable insight into the strategies employed by the central nervous system in the control of skilled activities.

Recently a few studies of the kinematic and dynamic aspects of multi-joint human and monkey arm movements have been conducted. The objective of these studies was to identify common kinematic features or stereotyped patterns of muscle activation characterizing these movements [Morasso 1981, Abend et al. 1982, Soechting & Lacquaniti 1981, Georgopoulos et al. 1981, Hollerbach and Flash 1982]. The planning and control of the kinematic aspects of arm movements is termed trajectory formation. The term trajectory refers to the configuration of the arm in space and to the speed of movement as the hand moves from its initial to its final position. Some investigators [Greene 1972, Soechting and Lacquaniti 1981, Saltzman 1979] have argued that trajectories are planned in joint variables. It has been claimed that the CNS uses a strategy of maintaining constant ratios between angular velocities of the joints in order to bring about a reduction in the complexity of the control problem by reducing the number of degrees of freedom. In contrast to this view, other investigators have argued that simplicity of motor control is achieved by planning hand trajectories in extracorporal space; joint rotations are then tailored to produce these desired hand movements [Lashley 1951, Bernstein 1967]. Recently, this view has gained support from studies of planar, unconstrained human and monkey movements [Morasso 1981, Abend et al. 1982, Georgopoulos 1981]. When moving the hand between pairs of targets subjects tended to generate roughly straight hand trajectories with single-peaked, bell-shaped speed profiles; this behavior was independent of the part of the work-space in which the movement was performed. Because the common invariant features of these movements were only evident in the extracorporal coordinates of the hand, these results are a strong indication that planning takes place in terms of hand trajectories rather than joint rotations.

Can this conclusion be generalised to more complex movements? When subjects were instructed to generate curved movements, the single-peaked hand speed profile was not

preserved. Although the hand paths appeared smooth, their curvature was not uniform, and the hand speed displayed one or more maxima. The minima between two adjacent speed peaks corresponded temporally to peaks in the curvature [Abend et al. 1982]. A similar temporal coupling between speed and curvature has been observed in handwriting, drawing [Viviani & Terzuolo 1980] and in infant reaching movements [von Hofsten 1979]. In this paper we will show that this behaviour can be derived from a single organising principle. This principle is based on the kinematics of the motion of the hand in extracorporal space, and provides further evidence that movements are planned in terms of hand trajectories rather than joint rotations.

To describe this behaviour, a mathematical model of the organization of voluntary arm movements is presented. There are, of course, many ways of formulating a mathematical description of any given phenomenon. In the work presented here, we have used dynamic optimization theory as it permits us to describe an assumed goal of this class of movements in a relatively simple formula, and derive from the formula a detailed prediction of the kinematics of a large number of specific movements. It will be shown that this mathematical model succeeds in accounting for the majority of the kinematic features of planar horizontal arm movements described in previous studies [Morasso 1981, Abend et al. 1982]. A number of new features of planar horizontal arm movements are also predicted by the model, and some new experimental results confirming these predictions are presented [Flash and Hogan 1982].

The Mathematical Model

Briefly, dynamic optimization requires the definition of a criterion function which describes the objective of the movement. Generally, this function is expressed mathematically as a time integral of a performance index, an algebraic function which may in general depend on the system inputs, outputs, and internal variables. A set of differential equations are formulated, which describe the response of the system to its inputs. The methods of variational calculus and optimal control theory are applied to find the trajectory which minimizes this criterion function subject to dynamic constraints imposed by the system differential equations and the algebraic constraints imposed at the end points, or during the motion. The use of optimization techniques to model natural behavior is appealing because of the analogy it bears to the optimization presumed to occur as a result of natural selection. Studies of two-joint arm movements have shown that as a result of practice the variability in hand trajectories is reduced exponentially with time [Georgopoulos et al. 1981]. The fact that only a few executed trajectories emerge, may indicate an underlying adaptive process tending to produce movements which optimize certain kinematic or dynamic variables

[Abend et al. 1982]. The critical step in the analysis is the selection of an appropriate objective function. Here the experimental results are suggestive. Since with learning and practice movements tend to be performed more smoothly and gracefully, this may indicate an underlying objective of achieving the smoothest movement which carries the hand from one equilibrium position to another. This was the point of departure of an optimization-based mathematical description of voluntary movements in monkeys [Hogan 1982, 1984, Bizzi et al. 1984]. The major qualitative and quantitative features of single-joint forearm movements have been successfuly predicted assuming that maximizing smothness may be equated to minimizing the mean-square jerk. Jerk is mathematically defined as the rate of change of acceleration. The work presented in this paper is the generalisation of that analysis to the case of multi-joint motion.

An important feature of the multi-joint case is that the predicted behavior depends critically on the choice of coordinates in which the criterion function is formulated. Our choice of coordinates was again guided by experimental observations, in particular the fact that the invariant features of upper limb movements are only evident when hand motion is expressed in extracorporal coordinates.

The position vector of the hand was defined with respect to a laboratory-fixed Cartesian coordinate system. Differentiating this position vector three times, Cartesian jerk for the hand can be defined. In moving from an initial to a final position in a given time t_f, the objective function to be minimized is the time integral of the square of the magnitude of jerk:

$$C = \frac{1}{2}\int_0^{t_f}\left((\frac{d^3x}{dt^3})^2 + (\frac{d^3y}{dt^3})^2\right)dt \qquad (1)$$

x and y are the time-varying hand position coordinates. Mathematical expressions for x(t) and y(t) are to be found, which bring the criterion function in equation 1 to a minimum.

This optimization procedure was used for the description of several experimentally observed types of human planar two-joint arm movements: unconstrained point-to-point movements, unconstrained curved movements and obstacle-avoidance movements. Comparisons of the mathematically predicted trajectories with experimental movement records were used to evaluate the success of the model.

Unconstrained Point-to-Point Movements

For unconstrained point-to-point movements the objective can be stated as follows:

"Generate the smoothest motion to bring the hand from the initial position to the final position in a given time."

One might expect the physical system which generates the movement (i.e. the neuro-musculoskeletal system) to impose certain constraints on the kinematic or dynamic variables. Such constraints might set limits on the hand speed or acceleration, due, for example, to limitations on the maximum torques that the system can generate or on how rapidly they can be changed [Nelson 1983]. However, none of the movements studied here was extremely fast nor did any of the movements require the generation of large forces. As the subjects did not operate anywhere near the limits of neuromuscular performance these constraints are inoperative. The optimization procedure is presented in Appendix A and results in a minimum jerk trajectory which is a fifth order polynomial in time for both x(t) and y(t).

If the constraints imposed by the physical system become important, the problem may be solved using the method of Pontryagin [Bryson & Ho 1975]. This method was also applied to our problem (Appendix B). The two methods yielded the same expressions for the hand trajectory.

The criterion function determines the form of the movement trajectory. The details are determined by the boundary conditions at the onset and termination of the movement. Given this information and the duration of the movement, the trajectory of the hand is specified in its entirety. No other information is required. Assuming the movement to start and end with zero velocity and acceleration, the following expressions for hand trajectory are obtained:

$$\begin{aligned} x(t) &= x_0 + (x_0 - x_f)(15\tau^4 - 6\tau^5 - 10\tau^3) \\ y(t) &= y_0 + (y_0 - y_f)(15\tau^4 - 6\tau^5 - 10\tau^3) \end{aligned} \tag{2}$$

where $\tau = t/t_f$ and x_0, y_0 are the initial hand position coordinates at $t = 0$.

Profiles of the predicted hand path (P) and hand tangential velocity (T) are shown in Figure 1A. The hand path, P, is illustrated by plotting the predicted hand location every 10 msec. T_1 to T_6 represent the targets. The plot of the predicted tangential velocity profile illustrates the hand speed, V, relative to the maximal speed, V_M, as a function of t/t_f , where t is the time and t_f is the movement duration. This trajectory is a straight line between initial and final positions with a bell-shaped unimodal velocity profile. Since the predicted trajectory depends only on the initial and final positions of the hand, it is invariant under translations and rotations. The shape of the predicted trajectory also does not change with amplitude or duration of the movement, which merely serve to change the scale of the position and time axes respectively. Note also that the expression describing the trajectory

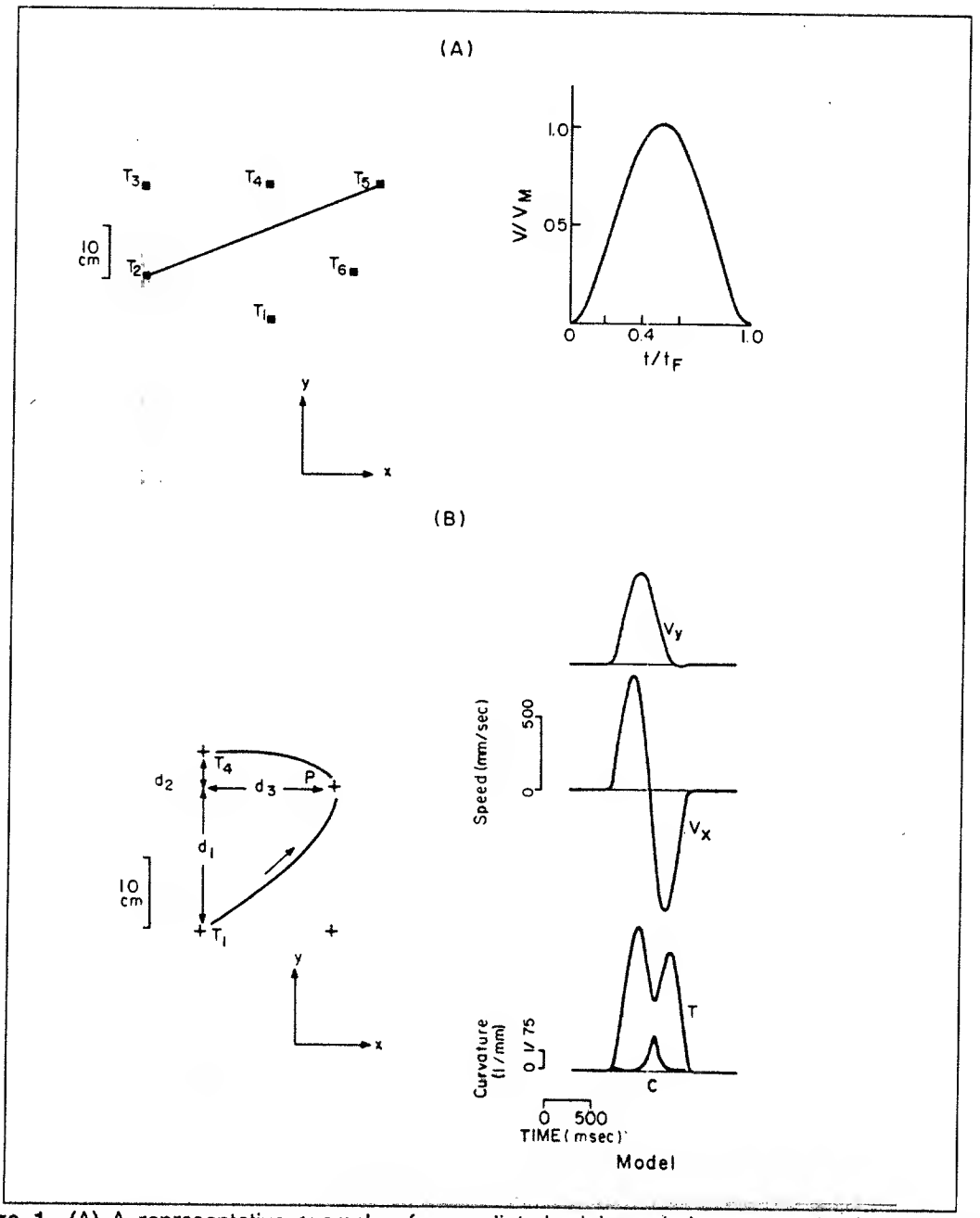

Figure 1 (A) A representative example of a predicted minimum-jerk unconstrained point-to-point hand trajectory. (B) A representative example of a predicted curved minimum-jerk hand trajectory between targets 1 and 4.

along the line joining the initial and final positions is a single fifth order polynomial in time which is identical to the minimum-jerk trajectory for single-joint motion [Hogan 1982, 1984].

Curved Point-to-Point Movements

To model curved and obstacle-avoidance movements, it was assumed that the hand is required, in its motion between the end points, to pass through a third specified point. Hence for these movements the movement objective can be stated as follows:

> "Generate the smoothest motion to bring the hand from the initial position to the final position in a given time. The hand must move to the final position through a specified point (a via point) at an unspecified time."

The requirement that the hand should move through a specified via point defines equality constraints; i.e., the hand position is prescribed at some intermediate time, t_1, between the onset and the termination of the movement. Hence, if the location of the via point with respect to a Cartesian coordinate system is given by the coordinates (x_1, y_1), the equality constraints on the hand position coordinates, x(t) and y(t), at time t_1, are:

$$\begin{aligned} x(t_1) &= x_1 \\ y(t_1) &= y_1 \end{aligned} \tag{3}$$

The time t_1 at which the hand has to pass through this point is not a priori specified but is derived from the optimization procedure. It is one of the predictions of the mathematical model. Problems of this kind are known as dynamic optimization problems with interior point equality constraints and techniques have been established for their solution [Bryson & Ho 1975]. The optimal trajectory for the entire movement between the initial and final position is derived in appendix C. For the particular problem treated here the technique used requires the continuity of the velocity and acceleration at this intermediate time. Since discontinuities of hand velocities and accelerations would require infinite accelerations and jerks, this is a reasonable requirement for arm movement. The details of the predicted movements, including the time at which the hand passes through the via point, depend on the chosen boundary conditions at time $t = 0$ and $t = t_f$ and on the specified interior point.

Applying the optimization technique one obtains an expression for the position component x(t) at all times $t \leq t_1$:

$$\begin{aligned} x^{-}(\tau) = \frac{t_f^5}{720}\Big(\pi_1\Big(\tau_1^4(15\tau^4 - 30\tau^3) + \tau_1^3(80\tau^3 - 30\tau^4) - 60\tau^3\tau_1^2 + 30\tau^4\tau_1 - 6\tau^5\Big) \\ + c_1\Big(15\tau^4 - 10\tau^3 - 6\tau^5\Big)\Big) + x_0 \end{aligned} \tag{4}$$

and for times $t \geq t_1$ the expression is:

$$x^+(\tau) = \frac{t_f^5}{720}\Big(\pi_1\Big(\tau_1^4(15\tau^4 - 30\tau^3 + 30\tau - 15) + \tau_1^3(-30\tau^4 + 80\tau^3 - 60\tau^2 + 10)\Big) + c_1\Big(-6\tau^5 + 15\tau^4 - 10\tau^3 + 1\Big)\Big) + x_f$$
$$= x^-(\tau) + \pi_1 \frac{t_f{}^5(\tau - \tau 1)^5}{120} \qquad (5)$$

These equations depend on the dimensionless variables $\tau_1 = t_1/t_f$ and $\tau = t/t_f$. Similar expressions are obtained for $y^+(\tau)$ and for $y^-(\tau)$ with constant coefficients, π_2 and c_2 replacing π_1 and c_1 in equations 4 and 5. These four coefficients, π_1, c_1, π_2 and c_2 which depend on the position coordinates at the boundaries and at the interior point and on t_1 are defined in Appendix C.

A typical predicted minimum-jerk curved movement is shown in Figure 1B. Displayed are the hand path (P) and the hand tangential velocity (T) and curvature (C) profiles. In addition, the two velocity profiles along the x axis, V_x, and the y axis, V_y, are also shown in Figure 1B. The meanings of d_1, d_2 and d_3 are explained in the text below. As this figure demonstrates, the predicted hand curvature increases, reaches a maximum, and then decreases again as the movement approaches the final position. The tangential velocity curve exhibits two peaks and the minimum in the tangential velocity curve occurs at the same time as the maximum curvature point. Again, the predicted trajectories are invariant under translation, rotation, time scaling and amplitude scaling.

Experimental Methods

To evaluate the model, simulated trajectories were compared to measured hand trajectories. Planar horizontal arm movements were recorded, using the apparatus shown in Figure 2. The subject was seated and held the handle of a two-link mechanical manipulandum. The shoulder was restrained throughout these experiments. The subject's wrist was braced in some of the trials, in others it was free to move. The subject was instructed to move the handle of the manipulandum under targets mounted on a horizontal plexiglass panel above the apparatus, upon their illumination. Visual information about the arm location was eliminated by darkening the room in which recordings took place. The joint angles of the mechanical apparatus were monitored by means of precision potentiometers. The potentiometer voltage signals were digitized at a rate of 100 samples per second and stored on magnetic tapes. These signals were filtered with an upper cut-off frequency of 5.2

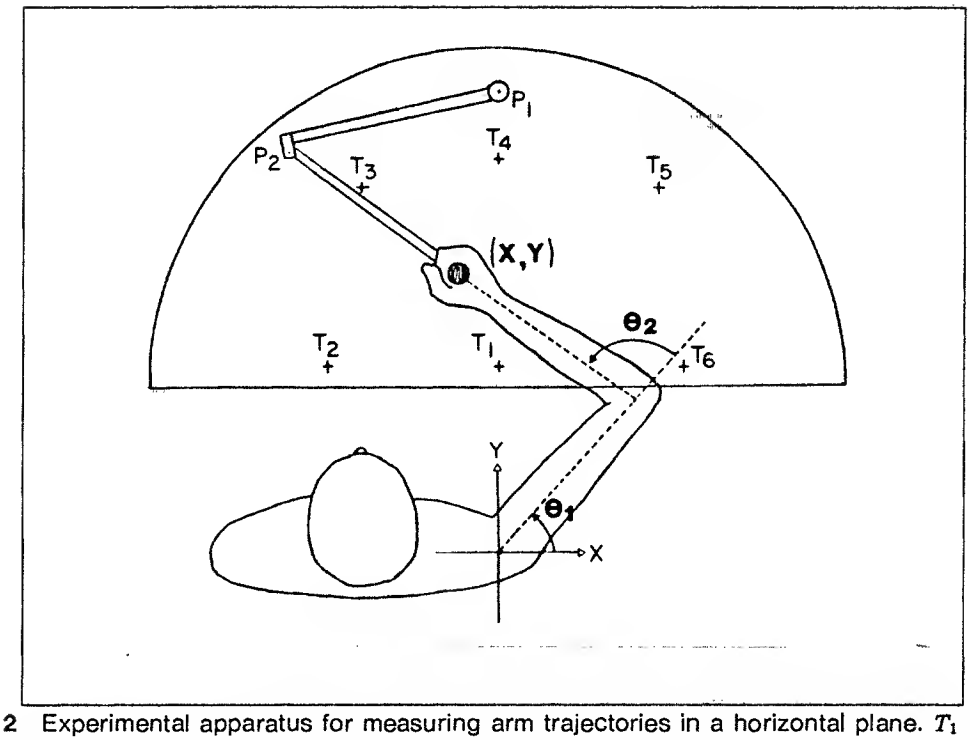

Figure 2 Experimental apparatus for measuring arm trajectories in a horizontal plane. T_1 to T_6 are the LED targets. θ_1 and θ_2 are respectively the subject's shoulder and elbow joint angles. Movement of the handle was measured by way of the potentiometers, P1 and P2.

Hz. A calibration procedure, executed before each experiment, determined the parameters for the conversion of these voltage signals to apparatus joint angles. Off-line data analysis was performed to compute the subject's hand position, and, based on the measured geometry of the subject's upper extremity, joint angles were also computed. Lagrange polynomial differentiation was used to obtain joint angular velocities, hand velocities and the curvature of the hand path. Handle movements as small as 1.0 mm could be detected and the error in the computed hand velocity was less than 4%. The error in computed hand curvature was less than 6%.

This apparatus and procedure are the same as used by Abend et al. [1982] and in this paper their results are compared to predictions of the mathematical model. The model also predicts several additional features of movement and to test these predictions new experiments were performed. Abend et al. used four experimental paradigms. In the first paradigm the subjects were instructed to move the hand from one target to another upon illumination of the second target. No instructions were given regarding the path between the two targets. We used the same experimental paradigm instructing the subjects to move at various speeds by specifying movement durations ranging from about 0.5 to 1.0 secs. In the second paradigm subjects were instructed to move the hand to a target along a self-generated curved path. No guide or obstacle was presented. In the third group of experiments, subjects were instructed to follow curved guides. These were constant

curvature arcs placed on top of the plexiglass panel. The fourth paradigm required obstacle avoidance. Subjects were instructed to move their hand from one target to another while avoiding an "obstacle" represented by a row of red light-emitting diodes. The maximum length of obstacles used in these experiments was 25 cm. The obstacle was placed between the targets with its long axis perpendicular to the line connecting the two targets.

In the above paradigms the subjects were not constrained to move the hand through any specific intermediate point on route to the target. We were therefore interested in determining what effect the introduction of a real via point would have on the movement. Experiments were conducted by us in which subjects were instructed to generate continuous movements from one target to another through an intermediate target. The intermediate target was lit throughout the movement. Movements involving the same set of three targets were performed at the subject's preferred speed first and then at a faster speed. Overall nine subjects participated in these experiments.

In most experiments the movements were confined to elbow and shoulder rotations in a horizontal plane at the subject's shoulder level. In some experiments, however, wrist movements were also allowed and/or subjects were instructed to move their arm in a horizontal plane passing through their waist.

To determine model-predicted trajectories for comparison, the values of several kinematic variables were derived from the experimental data. For straight trajectories, these values were the initial and final target locations and the movement durations. For unconstrained curved and obstacle avoidance movements, the location of the via point also had to be specified. This was determined from the location of the maximum curvature point. In experiments with an intermediate target, the location of the via point was taken to be the location of this target. These parameters were substituted in the polynomials derived from the dynamic optimization and hand positions were computed every 10 msec. These positions were then differentiated to derive hand velocities and differentiated again to derive hand accelerations and the curvature[1] was computed.

[1]Hand speed (T) and trajectory curvature (C) are defined as: $T = \sqrt{(\dot{x})^2 + (\dot{y})^2}$, and $C = \frac{\dot{x}\ddot{y} - \dot{y}\ddot{x}}{((\dot{x})^2 + (\dot{y})^2)^{\frac{3}{2}}}$ where $\dot{x}$, $\dot{y}$ are the hand velocity components and $\ddot{x}$, $\ddot{y}$ are the acceleration components.

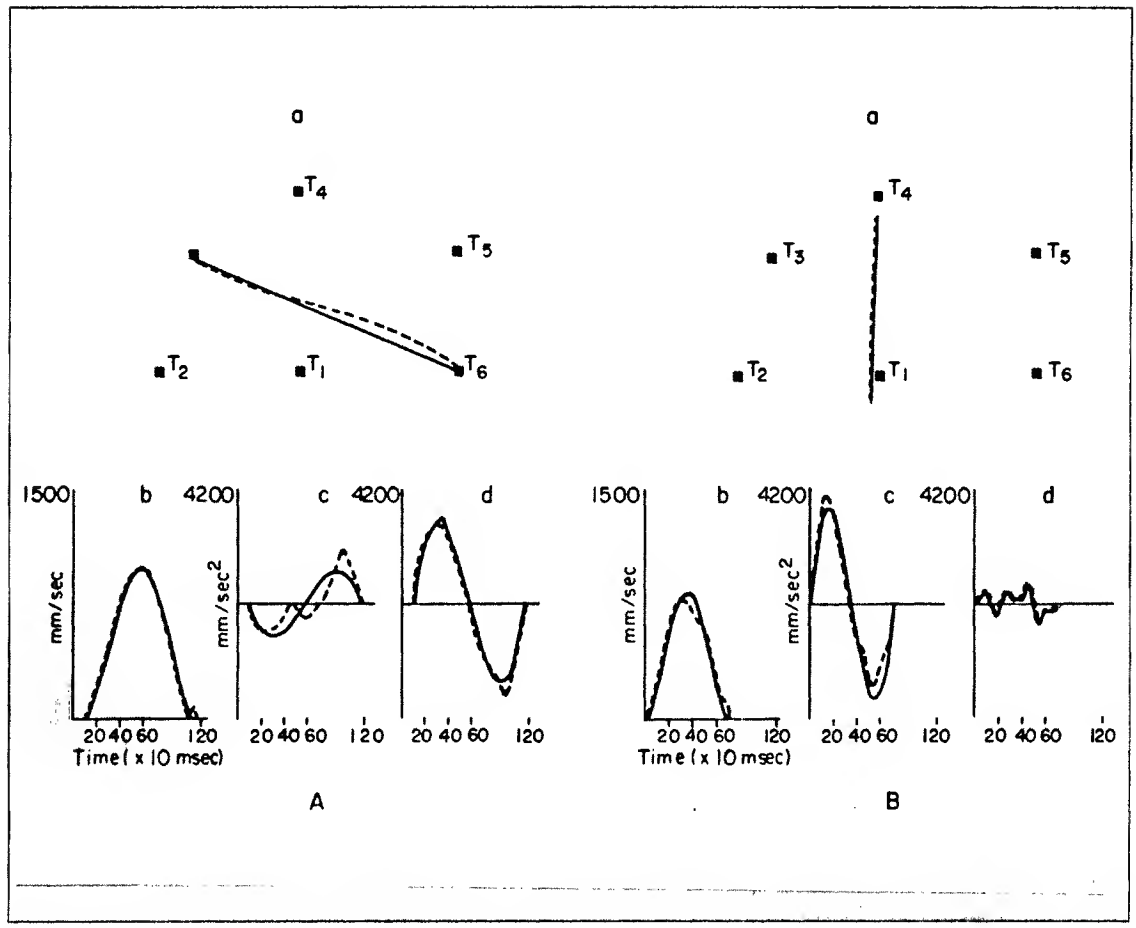

Figure 3 Overlapped predicted (solid lines) and measured (dotted lines) hand paths (a), speeds (b) and acceleration components along y axis (c), and along x axis (d) for two unconstrained point-to-point movements. (A) A movement between targets 3 and 6. (B) A movement between targets 1 and 4.

Results.

Typical experimental results for two unconstrained point-to-point movements are shown in Figure 3 superimposed on the predicted minimum-jerk trajectories for the same movements. As this figure shows, there is a good qualitative and quantitative match between the predicted and actual trajectories. There is a good agreement between the predicted and measured steepness of the rising and falling parts of the tangential velocity and acceleration curves, and the time at which maximum acceleration is reached. The predicted trajectory does not capture the asymmetry in the tangential velocity profile of the measured trajectory. The difference, however is quite small. There are also some slight discrepancies between the measured and predicted acceleration profiles.

Typical examples of the fit between the temporal behavior of real and simulated shoulder and elbow angles and angular velocities are shown in Figure 4. To obtain joint

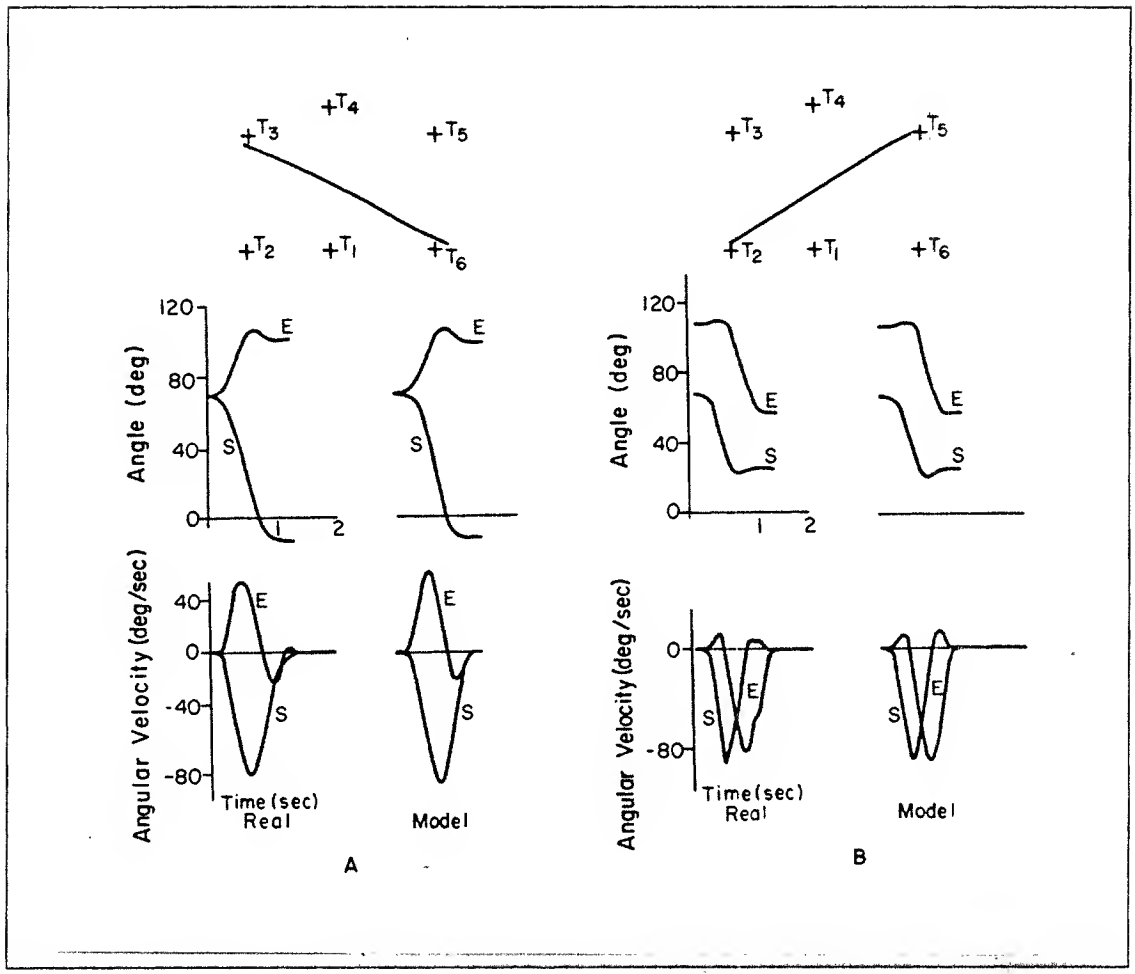

Figure 4 Measured and predicted shoulder, S, and elbow, E, joint angles and angular velocity profiles. (A) A movement between targets 3 and 6. (B) A movement between targets 2 and 5.

angles and angular velocities, the inverse kinematics problem [Brady et al. 1982] was solved. Since for horizontal planar two-joint movements hand trajectories uniquely define angular trajectories, this computation serves only to permit an additional comparison between the theoretical and experimental results. As can be seen in Figure 4 the actual and predicted angular velocity profiles agree quite well and there exist only minor discrepancies between the simulated and real trajectories.

A typical example for a predicted curved trajectory was shown above in Figure 1B. As this example demonstrates, the predicted trajectories display the majority of the observed features of real curved hand trajectories as discussed by Abend et al. [1982]. If real curved hand trajectories can be described adequately by the proposed model, they should display the kinematic features exhibited by the simulated trajectories. To facilitate the explanation of the nature of these predictions a simple geometric construction, shown in Figure 1B, is used. The movement end-points are connected by a straight line. The perpendicular to this line which passes through the via point is drawn. This second line, of length d_3, divides

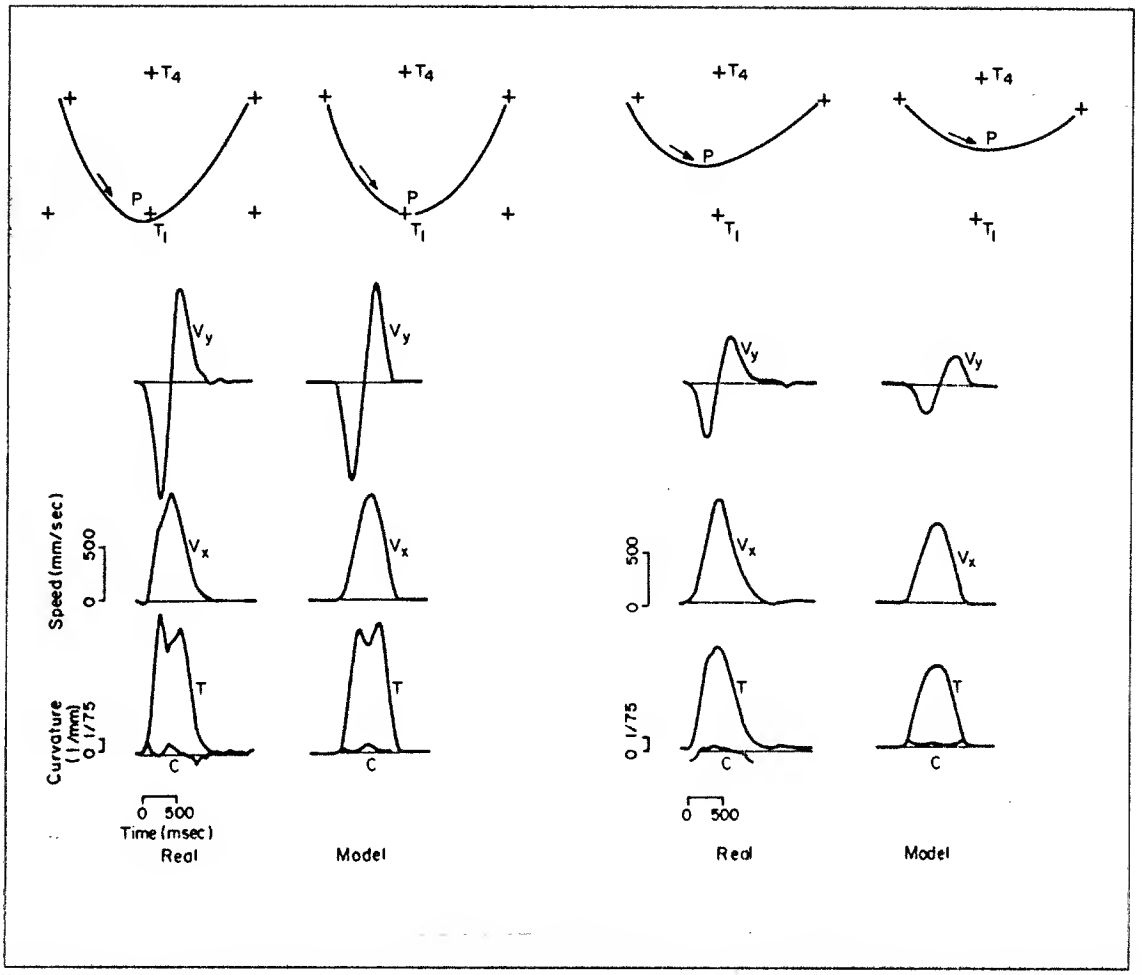

Figure 5 Representative examples of comparisons between measured (Real) and predicted (Model) trajectories from a "via-point" experiment in which the movement reversed its direction along the y axis. (A) The intermediate target was located at equal distances from the initial and final targets. (B) The intermediate target was at equal distances from the movement end-points but closer to the line connecting them.

the line connecting the two movement end-points into two segments of lenghts d_1 and d_2.

The first predicted kinematic feature relates to the dependency of the shape of the hand velocity and curvature profiles on the location of the via point. If the via point is displaced in any direction, towards either the initial or the final target, so that one of the two segments d_1 or d_2 is longer, the amplitude of the velocity peak on the corresponding portion of the movement will be higher. The second predicted kinematic feature relates to the depth of velocity valley, and the height of the curvature peak. For more highly curved movements the tangential velocity dip is more pronounced. Hence, for two movements of the same duration with the same values of d_1 and d_2, the amplitude of the hand curvature peak will be higher and the tangential velocity valley will be deeper for the movement with the larger value of d_3.

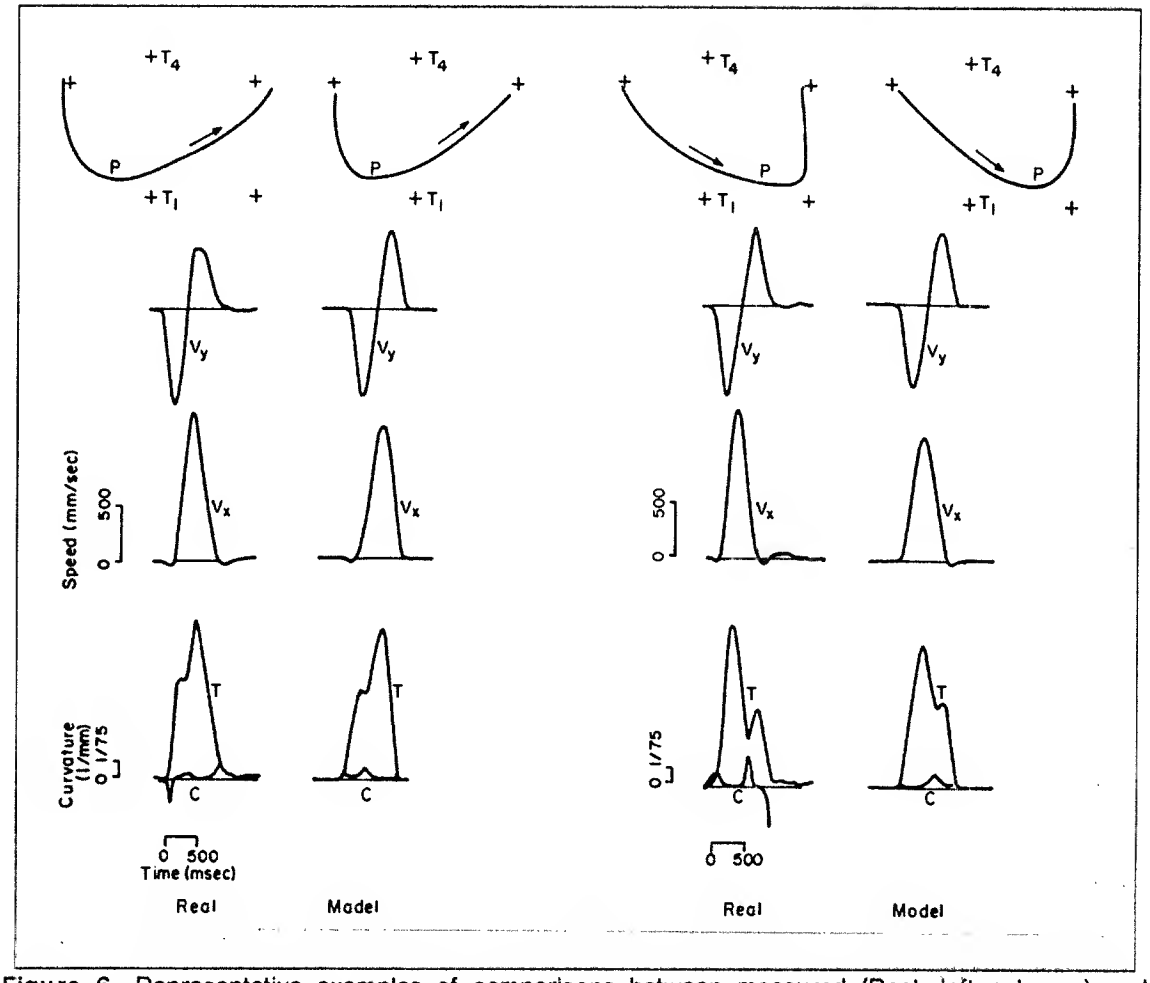

Figure 6 Representative examples of comparisons between measured (Real, left columns) and predicted (Model, right columns) trajectories from a "via-point" experiment in which the movement reversed its direction along the y axis. (A) The intermediate target was closer to the initial target. (B) The intermediate target was closer to the final target.

To test the validity of these two predictions, quantitatively simulated and measured hand trajectories were compared for movements through intermediate targets, unconstrained curved movements and obstacle-avoidance movements. In all the following figures measured hand paths (P), hand speed profiles (T), hand curvature profiles (C) and the profiles of the two velocity components along the two orthogonal axes (V_x and V_y) are displayed in the left column (Real) and the corresponding plots for the minimum jerk trajectories are displayed in the right column (Model). Comparisons of predicted and measured hand trajectories for arm movements generated by subjects in experiments with intermediate targets are shown in Figures 5-7.

Figures 5 and 6 describe results from trials in which the location of the via point, with respect to the initial and final targets, required the reversal of the direction of the hand movement along the y axis. In this group of movements, the intermediate target

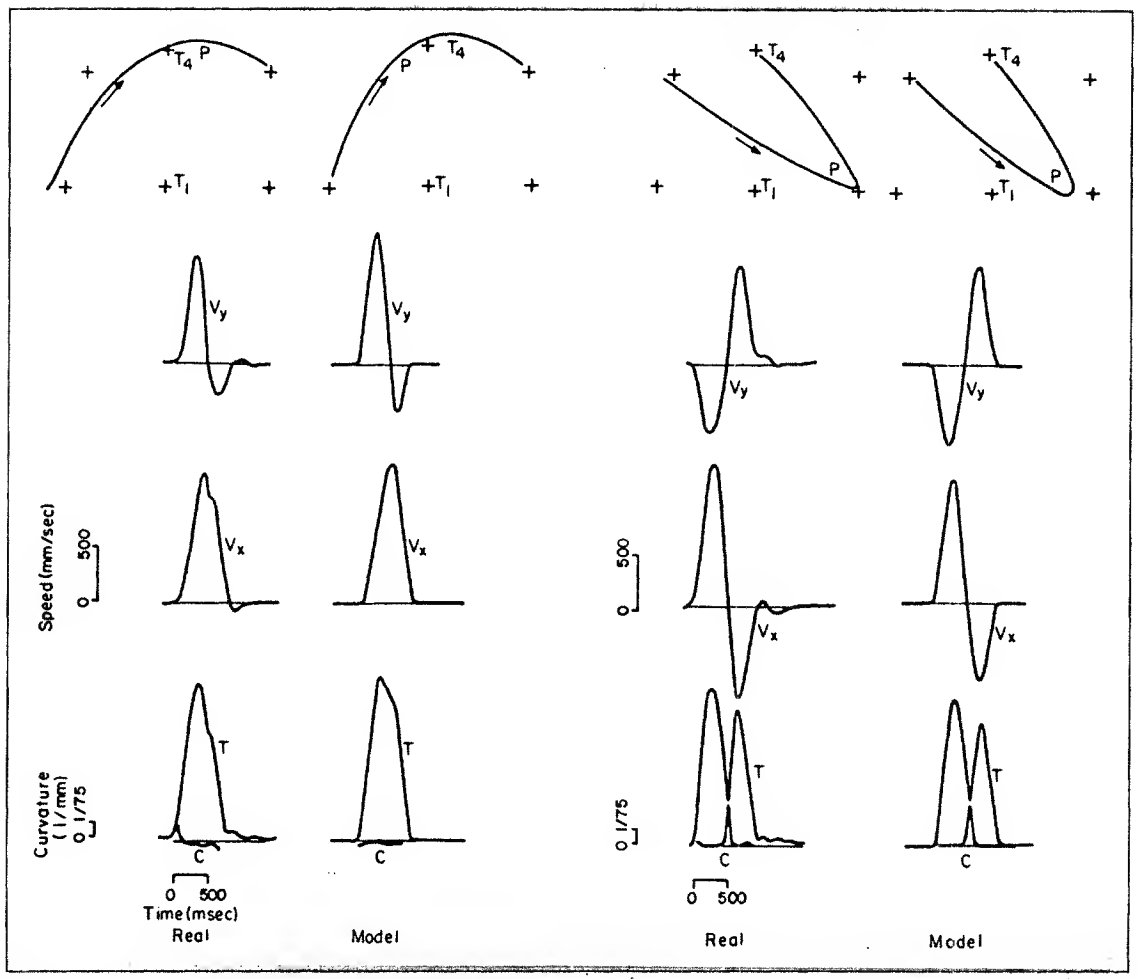

Figure 7 Representative examples of comparisons between measured (Real) and predicted (Model) trajectories from a "via-point" experiment in which the movement reversed its direction along both x and y axes.

was first placed at equal distances from the initial and final targets, closer to (Figure 5A) or further away (Figure 5B) from the line connecting these two targets, and then was symmetrically offset from the center in both directions along a line passing parallel to the y axis (Figure 6A and Figure 6B). As these figures show there is a good qualitative and quantitative fit between the measured and predicted trajectories. Furthermore, the measured hand trajectories validated the above predictions.

Figure 7 shows results from trials in which the locations of the intermediate targets required a reversal of movement direction along both the x and y axes. As this figure demonstrates, the fit of the predicted to the real trajectories was equally good under conditions of both translation and rotation of the movements.

Two obstacle-avoidance movements are compared to the corresponding simulated trajectories in Figure 8. Two unconstrained curved movements are compared to simulated trajectories in Figure 9. Again all of the above predicted features are exhibited. Note also the

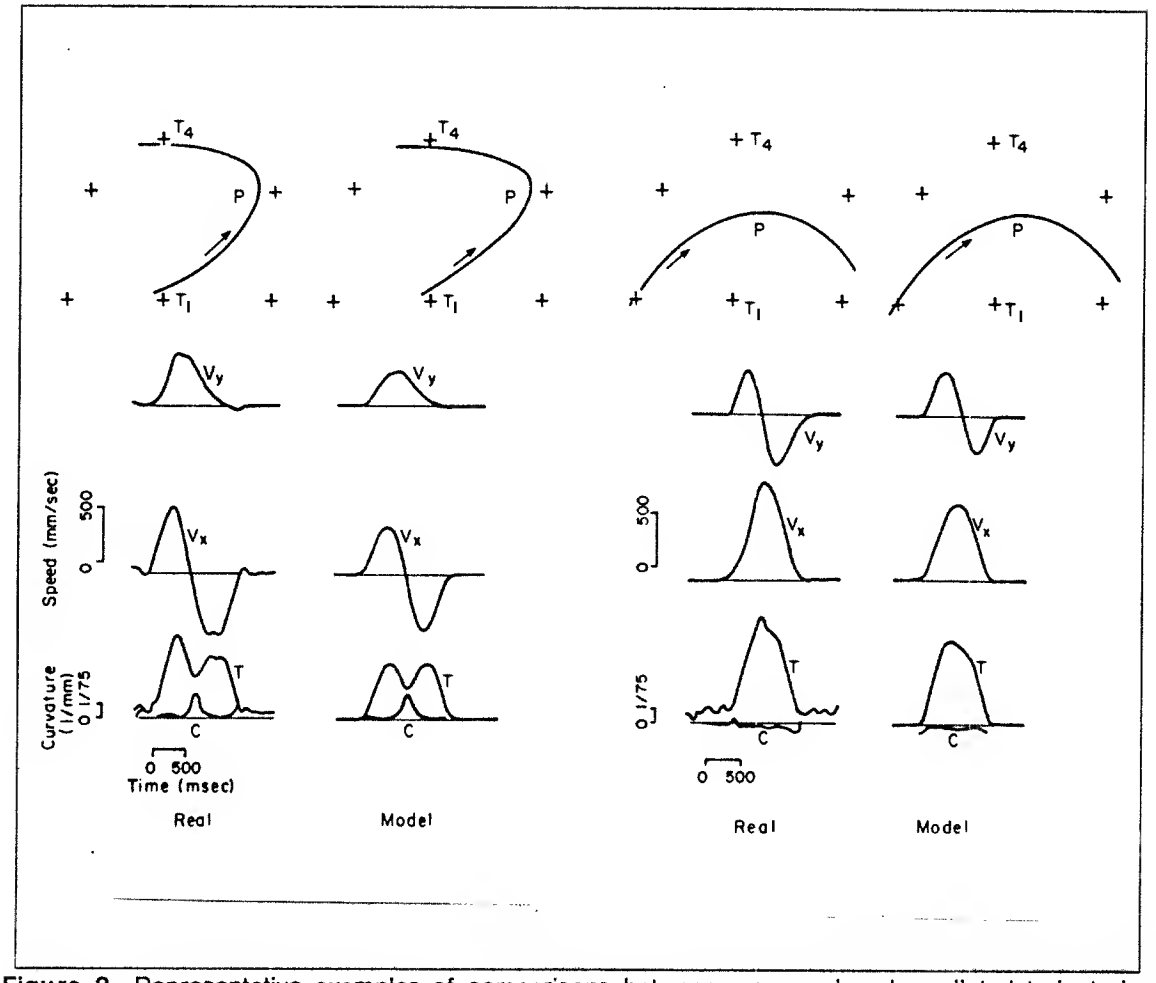

Figure 8 Representative examples of comparisons between measured and predicted trajectories for two obstacle-avoidance movements.

similarities in the kinematic characteristics of obstacle avoidance movements, unconstrained movements, and movements through intermediate targets.

Additional predictions can be made from the model. These are the "isochrony principle" and the scaling of the hand trajectories with speed. The isochrony principle states that the times it takes the hand to move along the two portions of the movement, from the start to the via point, and from the via point to the end of the movement, should be roughly equal, except for cases in which the via point is very close to either one of the movement end-points. Hence if $t_1/(t_1 + t_2)$ values are plotted versus $d_1/(d_1 + d_2)$ values, for several different movements, $t_1/(t_1 + t_2)$ should be expected to be roughly equal to 0.5 for most of $d_1/(d_1 + d_2)$ values between 0 and 1 except for $d_1/(d_1 + d_2)$ values quite close to 0 or 1. It is also predicted that for similar values of $d_1/(d_1 + d_2)$, the values of $t_1/(t_1 + t_2)$ will be independent of d_3. This behavior of the minimum-jerk trajectories is consistent with the differences in heights of the two velocity peaks on either sides of the velocity valley because, if the hand travels along both movement segments in roughly the same time, then

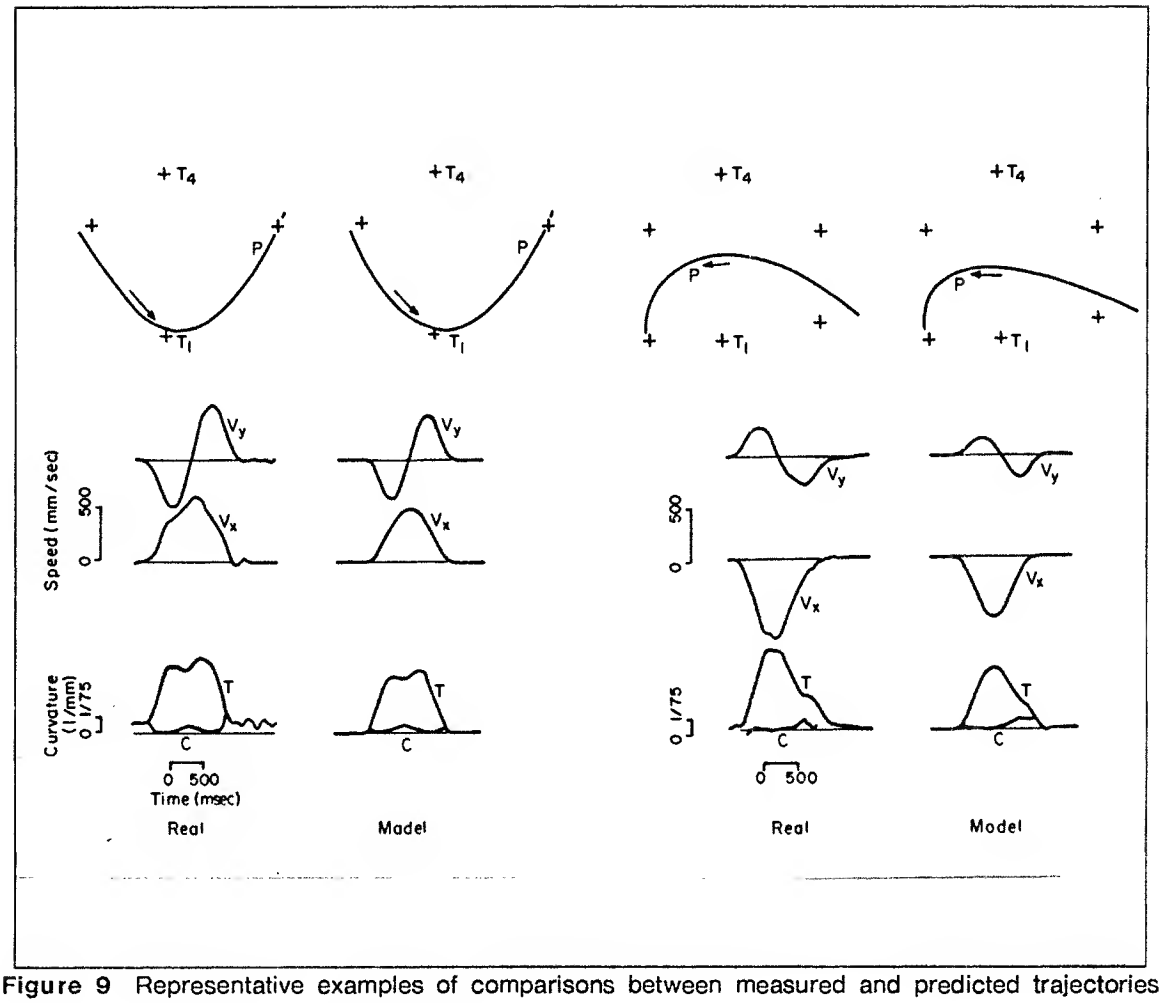

Figure 9 Representative examples of comparisons between measured and predicted trajectories for two unconstrained curved movements.

the velocity amplitude for the longer segment should be higher.

In Figure 10A, points corresponding to measured $t_1/(t_1 + t_2)$ values for various experimentally set $d_1/(d_1 + d_2)$ parameters, are superimposed on the predicted $t_1/(t_1 + t_2)$ versus $d_1/(d_1 + d_2)$ curve. The measured $t_1/(t_1 + t_2)$ values were derived from both unconstrained curved movements and movements through intermediate targets. Similarly, in Figure 10B points corresponding to measured $t_1/(t_1 + t_2)$ versus d_3 for various movements with similar values of $d_1/(d_1 + d_2)$, are superimposed on the corresponding predicted curve. In both figures the real points fall close to the predicted curves; within experimental errors the measured trajectories behave as predicted by the isochrony principle.

The predicted curved trajectories, like the straight trajectories, scale with time as the movement duration changes. Therefore, the path of the hand should be the same for fast and slow movements, while the hand speed throughout the movement should scale numerically by the ratio between the fast and slow movement durations. The scaling

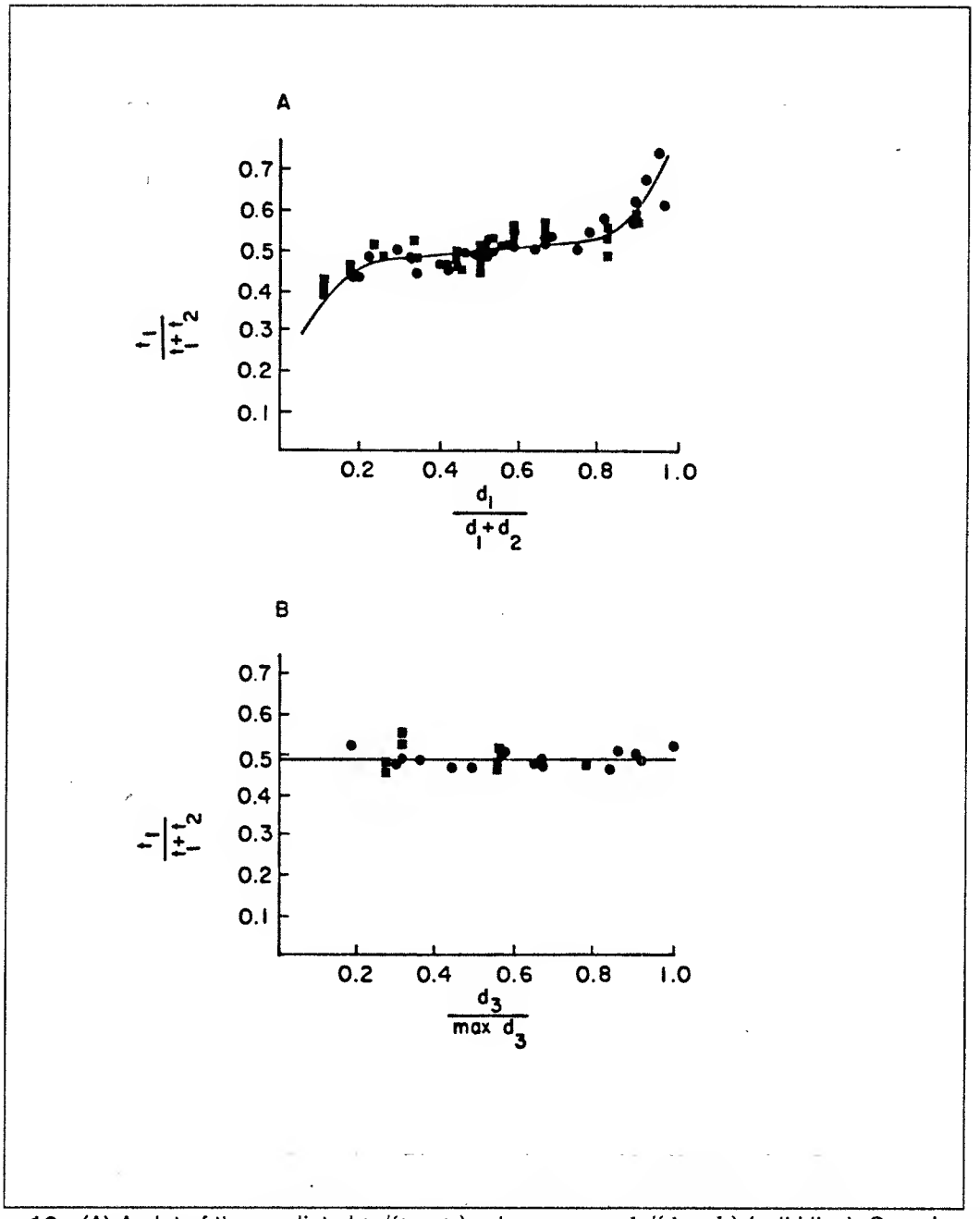

Figure 10 (A) A plot of the predicted $t_1/(t_1+t_2)$ values versus $d_1/(d_1+d_2)$ (solid line). Superimposed are measured $t_1/(t_1+t_2)$ values derived from unconstrained curved motions (circles), and from motions through intermediate targets (squares). (B) A plot of the predicted $t_1/(t_1+t_2)$ values versus d_3 (solid line). Superimposed are measured values derived from unconstrained curved motions (circles), and from motions through intermediate targets (squares).

prediction is validated by the measured movements as demonstrated in Figure 11A, in which the movement duration is 1.1 sec versus Figure 11B, with a movement duration of 0.85 sec. Moreover, as can be seen from this figure, the fact that the subjects move faster or slower does not affect the model performance.

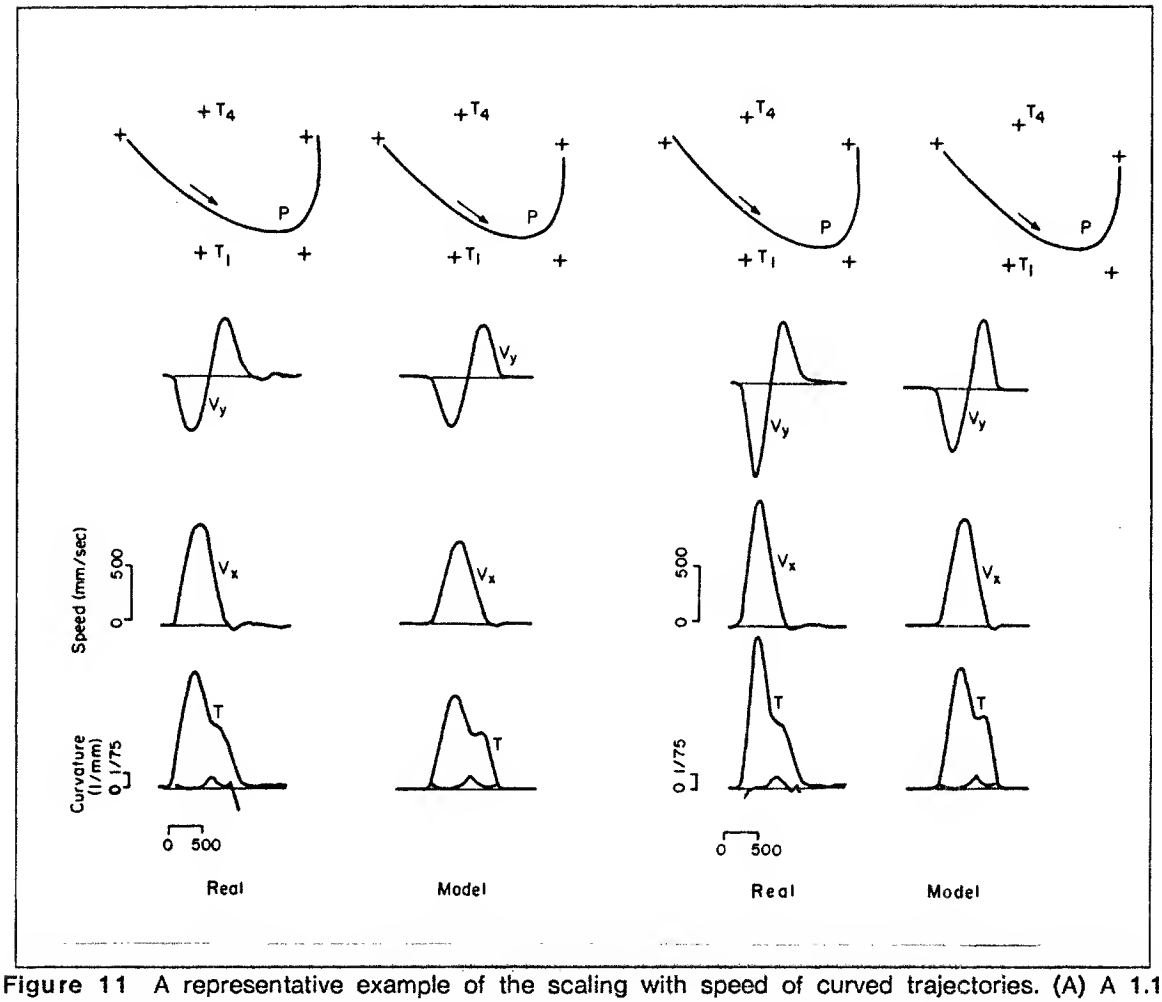

Figure 11 A representative example of the scaling with speed of curved trajectories. (A) A 1.1 sec. movement via an intermediate target. (B) A 0.85 sec. movement through the same targets.

The model predicts the same hand trajectories regardless of the specific joints involved in the generation of the movement or whether they are generated in a horizontal plane at the level of the subject shoulder or at other levels. This was found to be the case in the work of Abend et al. [1982]. Similarly, in our own experiments, in trials in which the hand brace was removed and rotations at the wrist joint were allowed, and in trials in which the movements were generated at a horizontal plane passing at the level of the subject 's waist, the trajectories were no different from the trajectories described in the above figures.

The model succeeds in accounting for the majority of the kinematic features of the real trajectories. A few fine-grained details of the real movements, however, were not captured in the simulated trajectories. These include, for example, the tendency of the first velocity peak to be higher than predicted, in movements between targets 1 and 4. Another example is the existence of irregularities in the hand path (the little "hooks") and hand speed as the hand approaches the goal target (e.g. Figures 7, 8).

Discussion.

The mathematical model presented in this paper matches observed human planar two-joint arm movements. The organisation of the movements was modelled through the criterion function. From the optimization of the criterion function explicit analytic expressions for the description of many different hand trajectories were derived. The derivation of these expressions depended on the specification of a small number of parameters; in the case of unconstrained point-to-point movements, only the movement duration and the position, velocity and acceleration at the end-points were required. Application of the same model to curved movements required only the addition of the position coordinates of a via point. In return, the model yielded the time at which the hand passes through the via point and a detailed time-history of the hand positions, velocities etc. The mathematical analysis, particularly the dynamic optimization methods used, bring about a dramatic reduction in the dimensionality of the problem of describing movement kinematics.

The mathematical model presented in this paper cannot be dismissed as merely elaborate curve fitting as it leads to several testable predictions: invariance of hand trajectories under translation and rotation in the workspace, scaling of hand trajectories with time and amplitude, temporal coupling between curvature and speed, and the "isochrony principle". All of these kinematic characteristics have been observed in the experiments reported in this paper and in the motor control literature. For example, it has repeatedly been observed that peak velocity increases as an approximately linear function of the distance to be traveled, so as to keep the duration of the movement roughly constant [Viviani & Terzuolo 1982]. Temporal coupling between hand curvature and speed has been previously described [Viviani & Terzuolo 1980, Abend et al. 1982] and movement scaling with time has also been observed for many different movements including two-joint arm movements, three dimensional reaching movements, handwriting, wrist movements etc. [Schmidt 1980].

How does the mathematical model presented here compare with alternative descriptions? Only a few models for the mechanisms underlying trajectory formation have been proposed. Given the tendency to generate roughly straight hand paths in point-to-point movements and the phenomenon of the temporal coupling of hand curvature and speed, Abend et al. [1982] and Viviani and Terzuolo [1982] have suggested that this phenomenon is due to a central mechanism which plans trajectories as sequences of movement segments which are then overlapped in time. Viviani and Terzuolo [1982] claim that movements obey an "isogony principle"; the ratio between tangential velocity and radius of curvature is piecewise constant. Our analysis of arm movements did not support this finding. Morasso and Mussa-Ivaldi [1982] suggest that curved movements are generated from separate strokes, each stroke characterized by various geometric parameters, such as length, total

angular change etc. Different movements may then be composed from different strokes, with different geometric parameters. Their model implies a need for storage and retrieval of strokes from a dictionary in memory; This dictionary would have to be very large.

These descriptions, however, do not make clear what rules and principles govern the choice of kinematic variables, nor why there is a tendency to generate straight paths in unconstrained movements in the first place. For example, the work by Morasso and Mussa-Ivaldi [1982], which suggests a computational model for trajectory planning, does not clarify what algorithm is used to overlap succeeding strokes in time nor does it suggest any explanation for the isochrony principle. By contrast, based on dynamic optimization of a single criterion function the model presented here accounted for the entire hand trajectory in both unconstrained and curved point-to-point movements. Furthermore, this model could be extended to describe more complicated movements by using more via points. However, a segmentation mechanism in the execution of hand trajectories is not ruled out by the optimization-based model and it is possible that such a mechanism underlies the planning of long and complicated sequences of movement. Whatever the planning process, the work presented here makes it clear that not every inflection point in the hand path nor every velocity valley necessarily imply the beginning of a new stroke. The success of the model presented here indicates that a more basic principle than mere segmentation underlies the specification of hand trajectories. Some evidence in support of this suggestion can be found in Wing's [1978] studies of handwriting in which it was shown that there exists a positive temporal correlation between the up and down strokes in the letter n, for example. This may indicate that an up-down stroke is planned as a single unit rather than two separate strokes.

This work also offers a plausible algorithm for Cartesian end-effector trajectory planning for artificial manipulators. Current methods of trajectory planning in robotics usually constrain the end-effector to follow straight lines using first order polynomials [Taylor 1979]. For more complicated movements or movements through via points, end-effector trajectories are planned as series of simple second-order polynomials which are smoothly joined together [Brady 1982] at knot points. While this method explicitly plans end-effector trajectories and assures that the end point will stay within the workspace it does not guarantee low values of jerk. By contrast the jerk minimization procedure presented here provides a rigorous way of planning trajectories of motions between equilibrium points and motions through via points while guaranteeing predictable and well-behaved trajectories.

The results presented here are independent of the physical system which generates the motion. No representation of the arm dynamics is required, nor is it necessary to make any assumption about the form of the neural input signals as in some other proposed models which attempt to account for movement kinematics [Zangenmeister et al. 1981].

Hence, the success of the model presented here supports the theories which view the motor system as being divided between higher levels which plan ideal trajectories for the end-effector, and lower level processes which translate them into torques and forces. These theories suggest that at higher levels there exists a kinematic representation of movement which does not take into account the mechanical nature of the actual effectors [Bernstein 1967].

The optimization model offers a new insight into these theories: the minimum-jerk movement is independent of the neuromuscular dynamics only if the demands of the movement lie within the capabilities of the neromuscular system. If one (or more) of the neuromuscular performance limits are reached, they impose a constraint on the achievable movements and the planning and execution processes cannot be clearly separated. However, dynamic optimization theory is sufficiently general to cover the case of performance-limited movements and may permit a prediction of the interaction between movement kinematics and neuromuscular dynamics as the limits of performance are approached, for example during fast movements.

During the movement of a multi-joint limb, the generation of appropriate joint torques for a trajectory is complicated by the presence of significant joint interactions due to inertial, centripetal, and.coriolis forces [Hollerbach and Flash, 1982]. Since these interaction effects are not present in the case of single-joint movements, strategies for the solution of dynamic problems for single-joint movements may not generalize to multi-joint movements. By contrast, the minimization of mean-squared jerk has been applied successfully to both single-joint [Hogan 1982, Hogan 1984] and multi-joint movements [Flash 1983]. By an appropriate choice of the boundary conditions (i.e the acceleration at the end of the motion is not constrained to be zero) the minimim-jerk model can also produce an excellent fit to observed repetetive movements [Nelson 1983]. Similarily, curved and straight hand movements were predicted here from the same criterion function while at the dynamic level each different movement requires very different patterns of joint torques. This indicates that a single unifying principle underlies the planning and the kinematic representation of all these movements. These results also indicate that at the higher levels a small number of general principles may be applied to the planning and coordination of movement kinematics, whereas at the lower levels less general strategies may be used to compensate for the difference in the dynamics of multi-jointed and single-jointed systems.

It is important to note that in the mathematical analysis presented here the minimum-jerk criterion function is expressed as the sum of the squares of the third derivatives of the coordinates of the hand in the extracorporal space. If the criterion function were expressed in joint coordinates (as the sum of squares of the third time-derivatives of the joint angles) the observed kinematic features and invariances in the hand trajectory would not be predicted.

Consequently, this work provides strong support for the hypothesis that movements are planned in terms of the motion of a "disembodied" hand moving in extracorporal space.

The concept of hierarchical motor planning [Saltzman 1979, Keele 1981] suggests also that same general and abstract internal representation of movement is used each time a movement is generated with temporal and spatial parameters chosen for that specific movement. Movement durations and spatial position cues were suggested as such specifiers [Keele 1981]. This would allow the CNS to use the same reference spatial coordinates for coding both visual information and motor actions and for learning, storage and retrieval of informaion in other skills such as drawing or handwriting. The minimum-jerk model is completely consistent with this hypothesis. The information necessary to obtain a detailed specification of the trajectory of the hand between the two targets was the movement duration and the extracorporal (e.g. Cartesian) locations of the targets.

The fact that hand trajectories are seldom performed twice in exactly the same way can be used to argue that different rules are used each time a movement is generated. Such variability in hand trajectories generated by different subjects or the same subject on succeeding trials may however be due to slight changes in the perceived locations of points in space to which the hand moves, or through which it passes. Another possible source of movement variability might be motor variability, since the final product depends on the translation of the motor plan into muscular activity and on the interaction of the arm with the environment [Keele 1981].

Accordingly, one physiological interpretation for the qualitative and quantitative fit of the experimentally recorded movements to minimum-jerk movements is that the CNS explicitly uses a trajectory planning strategy, which is captured by the mathematical model presented here, in order to translate task objectives, coded by exteroceptive position cues, into trajectory plans. An alternative explanation is that the smoothness of hand trajectories is an outcome of the intrinsic properties of the neural and muskuloskeletal hardware. This alternative explains the observations at the level of the neuromuscular structure rather than at the level of higher cognitive processes, but the basic principle is the same: that evolutionary adaptations have led to an optimization of biological movements. However, as mentioned above, the model presented here is based on the jerk of the hand in extracorporal coordinates and is unsuccessful when expressed in joint angles. Therefore, it can be argued that the smoothness of contraction of individual muscles cannot be the cause of the agreement between theory and experiment.

The rationale for jerk minimization in biological trajectory planning does not lend itself to self-evident, casual explanations. Given the fact that the movements under consideration occur at moderate speeds and do not subject the system to undue stress, it is unlikely that such a strategy has evolved to minimize the "wear and tear" on the system. It is possible

that the objective is to minimize unwanted, abrupt changes in the forces transmitted to objects carried by the hand. Another possibility [Hogan 1984] is that the objective is to maximize the predictability of the trajectory, which is consistent with minimizing its higher time-derivatives. To discriminate between these and other possiblities will require further work.

Finally, it is not suggested that minimization of jerk is the single objective underlying all movements. Minimization of mean-squared jerk is a mathematical model of one movement objective, the production of smooth, graceful movements. Alternatives such as the minimization of mean-squared acceleration and mean-squared snap (the fourth time-derivative of position) have been explored [Flash 1983]. This analysis has demonstrated that the minimization of mean-squared acceleration results in parabolic tangential velocity profiles and non-zero accelerations at the movement end-points, unlike the actual movements. On the other hand minimization of mean-squared snap provides a good fit to the observed experimental data. The limited resolution of the experimental data, however, has not allowed us to establish unequivocally which one of the two models, jerk minimization or snap minimization, offers a better fit. Further pursuit of the question of what objectives are optimized in human movements may help in clarifying what other principles underly motor planning [Pew and Baron 1978].

References

1. Abend, W., Bizzi, E., Morasso, P., "Human arm trajectory formation.," Brain 105 (1982), 331-348.

2. Bernstein, N., The Coordination and Regulation of Movements. , Pergamon Press., Oxford, 1976.

3. Bizzi, E., Accornero N., Chapple W., Hogan N.o, "Posture Control and Trajectory Formation During Arm Movement," J. Neurosci. (1984), in press.

4. Brady, M., "Trajectory Planning," In Robot motion: planning and control, MIT Press, Cambridge, Mass (1982), 221-244.

5. Brady, J. M., Hollerbach, J. M., Johnson, T. L., Lozano-Perez, T., Mason, M. T., eds., Robot Motion: Planning and Control , MIT Press, Cambridge, Mass., 1982.

6. Bryson, A.E, Ho, Yu-Chi., Applied Optimal Control. , Hempshire Publ. Co., 1975.

7. Clark, M.R, Stark, L., "Time optimal behavior of human saccadic eye movement.," IEEE Trans. on Automatic Control AC-20 (1975), 345-348.

8. Flash, T., Hogan, N., "Evidence for an optimization strategy in arm trajectory formation," Abst. 12th Neuroscience, Minneapolis, Minnesota (1982).

9. Flash, T., Organizing principles underlying the formation of hand trajectories, Ph. D. Thesis, Harvard/MIT Division of Health Sciences and Technology, 1983.

10. Georgopoulos, A.P., Kalaska, J.F., Massey, J.T., "Spatial trajectories and reaction times of aimed movements: Effects of practice, uncertainty, and change in target location.," J. Neurophysiol. 46 (1981), 725-743..

11. Granit, R., "Comments on history of motor control.," In: Handbook of Physiology, Section 1: The Nervous System. Volume 2: Motor Control, V.B. Brooks (ed.), Williams and Wilkins, Baltimore (1981), 1-16.

12. Greene, P.H., "Problems of organization of motor systems.," In: Progress in theoretical biology, Rosen, R., Snell, F. (eds.) Academic Press, New York (1972).

13. Hogan, N., "Control and coordination of voluntary arm movements.," Proc. American Control Conf. (1982).

14. Hogan, N., "An organizing principle for a class of voluntary movements," J. Neurosci. (1984), in press.

15. Hollerbach, J. M., Flash, T., "Dynamic interactions between limb segments during planar arm movement," Biol. Cybern. 44 (1982), 67-77.

16. Keele, S.W., "Behavioral analysis of movement.," In: Handbook of Physiology, Section 1: The Nervous System. Volume 2: Motor Control, V.B. Brooks (ed.), Williams and Wilkins, Baltimore (1981), 1391-1414.

17. Lashley, K.S, "The Problem of serial order in behaviour.," In: Cerebral mechanisms in behavior. L.A. Jeffress (ed.), Wiley, New York (1951), 112-146.

18. Morasso, P., "Spatial control of arm movements," Exp. Brain Res. 42 (1981), 223-227.

19. Morasso, P., Mussa-Ivaldi, F.A., . "Trajectory formation and handwriting: a computational model.," Biol. Cybern. 45 (1982), 131-142.

20. Nelson, W., "Physical principles for economies of skilled movements," Biol. Cybern. 46 (1983), 135-147.

21. Pew, R.W., Baron, S., "The component of an information processing theory of skilled performance based on optimal control perspective.," In: information Processing in Motor Control and Learning. G.E. Stelmach (ed.), Academic Press, New York (1978), 153-172.

22. Pontryagin, L.S., Boltyanskii, V., Gamkrelidze, R. and Mishchenko, E., The mathematical theory of optimal processes. , Interscience Publishers, Inc., New York., 1962.

23. Schmidt, R.A., Zelaznick, H.N., Frank, J.S., "Sources of inaccuracy in rapid movement.," In: Information Processing in Motor Control and Learning. G.E. Stelmach (ed.), Academic Press, New York (1978), 183-203..

24. Schmidt R.A., "On the theoretical status of time in motor program representations.," In :Tutorials in motor behavior. G.E. Stelmach (ed.), North-Holland, Amsterdam (1980).

25. Soechting, J. F., Lacquaniti, F., "Invariant characteristics of a pointing movement in man," J. Neurosci. 1 (1981), 710-720.

26. Soechting, J. F., Lacquaniti, F., "Modification of trajectory of a pointing movement in response to a change in target location," J. Neurophysiol. 49 (1983), 548-564.

27. Stein, R.B, "What muscle variable(s) does the nervous system control in limb movements," The Behavioral and Brain Sciences 5, 4 (1982), 535-578.

28. Taylor, R. H., "Planning and execution of straight-line manipulator trajectories," IBM J. Res. Develop. 23 (1979), 424-436.

29. Viviani, P. and Terzuolo, C., "Space-time invariance in motor skills.," In: Tutorials in Motor Behavior. Stelmach, G.E, Requin, J. (eds.), North-Holland, Amsterdam (1980), 525-533..

30. Viviani, P. and Terzuolo, C., "Trajectory determines movement dynamics," Neurosci. 7 (1982), 431-437.

31. von Hofsten, C., "Development of visually directed reaching: the approach phase.," J. Human Movement Studies 5 (1979), 160-178.

32. Wing, A.M., "Response timing in handwriting.," In: information Processing in Motor Control and Learning. G.E. Stelmach (ed.), Academic Press, New York (1978), 153-172.

33. Zangenmeister, W.H., Lehman, S., Stark, L., "Simulation of head movement trajectories: Model and fit to main sequence.," Biol. Cyber. 41 (1981), 19-23.

Appendices.

The optimization procedures used in this work are described in the following appendices. A comprehensive introduction to dynamic optimization and variational calculus is found in Bryson and Ho [1975] and Pontryagin et al. [1962].

Appendix A: Unconstrained Optimization.

Unconstrained point-to-point movements.

We want to minimize the following objective function:

$$C = \frac{1}{2}\int_0^{t_f} ((\frac{d^3x}{dt^3})^2 + (\frac{d^3y}{dt^3})^2)\,dt \qquad (A1)$$

Generally, for any function x(t), which is sufficiently differentiable in the interval $0 \leq t \leq t_f$, and for any performance index $L[t, x, \dot{x}, \ddot{x}, ...\frac{d^n x}{d^n t}]$ which is integrable over the same interval, the unconstrained cost function:

$$C(x(t)) = \int_0^{t_f} L[t, x, \dot{x}, \ddot{x}, ...\frac{d^n x}{d^n t}]\,dt \qquad (A1)$$

assumes an extremum when x(t) is the solution of Euler-Poisson equation:

$$\frac{\partial L}{\partial t} - \frac{d}{dt}(\frac{\partial L}{\partial \dot{x}})..... + (-1)^n \frac{d^n}{dt^n}\frac{\partial L}{\partial(^n x)} = 0 \qquad (A2)$$

Since in our case

$$L = \frac{1}{2}((\ddot{x})^2 + (\ddot{y})^2) \qquad (A3)$$

we get the equation

$$\frac{d^3}{dt^3}(\frac{\partial \dot{x}^2}{\partial \ddot{x}}) + \frac{d^3}{dt^3}(\frac{\partial \dot{y}^2}{\partial \ddot{y}}) = 0 \qquad (A4)$$

We can uncouple the terms depending on the two position components to get:

$$\frac{d^6x}{dt^6} = 0 \qquad \frac{d^6y}{dt^6} = 0 \qquad (A5)$$

The resulting solution to differential equations of this kind is given by a fifth order polynomial:

$$\begin{aligned} x(t) &= a_0 + a_1 t + a_2 t^2 + a_3 t^3 + a_4 t^4 + a_5 t^5 \\ y(t) &= b_0 + b_1 t + b_2 t^2 + b_3 t^3 + b_4 t^4 + b_5 t^5 \end{aligned} \qquad (A6)$$

Appendix B: Dynamic Optimization.

The optimization method.

Generally, optimization problems similar to the problem solved here, involve a system which can be described by a set of nonlinear differential equations:

$$\dot{\underline{s}} = f[\underline{s}(t), \underline{u}(t), t] \tag{B1}$$

where $\underline{s}(t)$ is a n vector function of state variables and $\underline{u}(t)$ is a m vector control function. The problem is to find the control $\underline{u}(t)$ which in carrying the system from an initial state $\underline{s}(0)$ to a final state $\underline{s}(t_f)$, the cost function C(t) is optimized. C(t) is defined as:

$$C(t) = \int_0^{t_f} L[\underline{s}(t), \underline{u}(t), t]\, dt \tag{B2}$$

where $L[\underline{s}(t), \underline{u}(t), t]$ is the performance index.

This problem can be solved by the method of Pontryagin [Pontryagin et al. 1962]. One defines a n component co-state (Lagrange multipliers) vector $\underline{\lambda}(t)$ and a scalar Hamiltonian:

$$H[\underline{s}(t), \underline{u}(t), t] = L[\underline{s}(t), \underline{u}(t), t] + \underline{\lambda}^T(t) f[\underline{s}(t), \underline{u}(t), t] \tag{B3}$$

The following differential equations define the necessary conditionns for a minimum to exist:

$$\dot{\underline{s}}(t) = \underline{f}(\underline{s}(t), \underline{u}(t), t) \tag{B4}$$

$$\dot{\underline{\lambda}}(t) = -\frac{\partial H}{\partial \underline{s}} \tag{B5}$$

$$\frac{\partial H}{\partial \underline{u}} = 0 \tag{B6}$$

Unconstrained point-to-point movements.

For our problem we define a state vector $\underline{s}^T(t) = [x, y, u, v, z, w]$ and a control vector $\underline{u}^T(t) = [\delta, \gamma]$.

The components of these vectors are defined by the system equations:

$$\begin{aligned}
\dot{x} &= u \\
\dot{y} &= v \\
\dot{u} &= \ddot{x} = z \\
\dot{v} &= \ddot{y} = w \\
\dot{z} &= \dddot{x} = jerk_x = \delta \\
\dot{w} &= \dddot{y} = jerk_y = \gamma
\end{aligned} \tag{B7}$$

and the Hamiltonian is:

$$H = \lambda_x u + \lambda_y v + \lambda_u z + \lambda_v w + \lambda_z \delta + \lambda_w \gamma + \frac{1}{2}(\gamma^2 + \delta^2) \tag{B8}$$

The necessary conditions for a minimum to exist are:

$$\begin{aligned} -\frac{d\lambda_x}{dt} &= 0 \\ -\frac{d\lambda_y}{dt} &= 0 \\ -\frac{d\lambda_u}{dt} &= \lambda_x \\ -\frac{d\lambda_v}{dt} &= \lambda_y \\ -\frac{d\lambda_z}{dt} &= \lambda_u \\ -\frac{d\lambda_w}{dt} &= \lambda_v \end{aligned} \tag{B9}$$

The necessary conditions on the control variables are:

$$\begin{aligned} \frac{\partial H}{\partial \delta} &= \delta + \lambda_z = 0 \\ \frac{\partial H}{\partial \gamma} &= \gamma + \lambda_w = 0 \end{aligned} \tag{B10}$$

Applying the following boundary conditions:

$$\begin{aligned} x(0) &= x_0 \quad & y(0) &= y_0 \\ x(t_f) &= x_f \quad & y(t_f) &= y_f \\ u(0) &= 0 \quad & u(t_f) &= 0 \\ v(0) &= 0 \quad & v(t_f) &= 0 \\ z(0) &= 0 \quad & z(t_f) &= 0 \\ w(0) &= 0 \quad & w(t_f) &= 0 \end{aligned} \tag{B11}$$

We solve these equations and get the following fifth order polynomials for the position coordinates x(t) and y(t):

$$\begin{aligned} x(t) &= a_0 + a_1 t + a_2 t^2 + a_3 t^3 + a_4 t^4 + a_5 t^5 \\ y(t) &= b_0 + b_1 t + b_2 t^2 + b_3 t^3 + b_4 t^4 + b_5 t^5 \end{aligned} \tag{B12}$$

Appendix C: Via Point Constrained Optimization

Problems with interior point equality constraints.

For curved movements we assumed that the hand is constrained to pass through the via point at time t_1 and the coordinates of this point are x_1 and y_1. Problems of this kind

are defined as *optimal control problems with interior point equality constraints on the state variables* [Bryson & Ho, 1975].

For such problems one has a set of constraints at some time t_1:

$$\underline{N}(\underline{s}(t_1), t_1) = \mathbf{0} \tag{C1}$$

where $\underline{N}$ is a q-component vector function. These interior point constraints can be augmented to the cost function by a Lagrange multiplier vector $\underline{\pi}$ so that the new cost function is:

$$C = \underline{\pi}^T \underline{N} + \int_0^{t_f} (H - \underline{\lambda}^T \dot{\underline{s}}) \tag{C2}$$

The solution is obtained by allowing discontinuities in the co-state variables (Lagrange coefficients) $\underline{\lambda}(t)$'s and in the Hamiltonian $H[t, \underline{\lambda}(t), \underline{s}(t)]$. One can define a vector of Lagrange coefficients $\underline{\lambda}^+(t)$ and Hamiltonian $H^+(t)$ for $t \geq t_1$ and a vector $\underline{\lambda}^-(t)$ and Hamiltonian H^- for $t \leq t_1$. At time t_1 these variables satisfy the equations:

$$\underline{\lambda}^-(t_1) = \underline{\lambda}^+(t_1) + \underline{\pi}^T \frac{\partial \underline{N}}{\partial \underline{s}(t_1)} \tag{C3}$$

$$H^-(t_1) = H^+(t_1) - \underline{\pi}^T \frac{\partial \underline{N}}{\partial t_1} \tag{C4}$$

The q components of $\underline{\pi}$ are determined by the constraint equations (C1) while time t_1 is fully determined by equation (C4).

Minimum-jerk trajectories with via point constraints.

For our specific problem the only constraints are on hand position along both axes at time t_1:

$$\begin{aligned} x(t_1) &= x_1 \\ y(t_1) &= y_1 \end{aligned} \tag{C5}$$

The Hamiltonian H^- for all times, such that $t \leq t_1$ is:

$$\begin{aligned} H^- =& \lambda_x^- u^- + \lambda_y^- v^- + \lambda_u^- z^- + \lambda_v^- w^- + \lambda_z^- \delta^- + \lambda_w^- \gamma^- \\ &+ \frac{1}{2}((\gamma^-)^2 + (\delta^-)^2) \end{aligned} \tag{C6}$$

and the Hamiltonian H^+ for times $t \geq t_1$ is:

$$\begin{aligned} H^+ =& \lambda_x^+ u^+ + \lambda_y^+ v^+ + \lambda_u^+ z^+ + \lambda_v^+ w^+ + \lambda_z^+ \delta^+ + \lambda_w^+ \gamma^+ \\ &+ \frac{1}{2}((\gamma^+)^2 + (\delta^+)^2) \end{aligned} \tag{C7}$$

Since the only constraint equations relate to position the only discontinuities are in λ_x and λ_y and, therefore, according to equation (C3), we get :

$$\begin{aligned} \lambda_x^- &= \lambda_x^+ + \pi_1 \\ \lambda_y^- &= \lambda_y^+ + \pi_2 \end{aligned} \tag{C8}$$

while all the other Lagrange coefficients are continuous at $t = t_1$:

$$\begin{aligned} \lambda_u^+(t_1) &= \lambda_u^-(t_1) \\ \lambda_v^+(t_1) &= \lambda_v^-(t_1) \\ \lambda_z^+(t_1) &= \lambda_z^-(t_1) \\ \lambda_w^+(t_1) &= \lambda_w^-(t_1) \end{aligned} \tag{C9}$$

Since time t_1 is not explicitly specified, the Hamiltonian must be continuous at t_1 as emerges from equation (C4) :

$$H^+(t_1) = H^-(t_1) \tag{C10}$$

Next we write the necessary conditions for the existence of a minimum. These equations are derived separately for $t \geq t_1$ and $t \leq t_1$. In addition we require continuity of velocities and accelerations at t_1, so that:

$$\begin{aligned} u^+(t_1) &= u^-(t_1) \\ v^+(t_1) &= v^-(t_1) \\ z^+(t_1) &= z^-(t_1) \\ w^+(t_1) &= w^-(t_1) \end{aligned} \tag{C11}$$

These come as a result of the requirements of the optimization technique for continuity of the state variables at the interior points [Bryson & Ho, 1975].

Solving the equations, defining the necessary conditions for a minimum and applying the boundary conditions at $t = t_0$ and at $t = t_f$, one obtains an expression for x(t) at all times $t \leq t_1$:

$$\begin{aligned} x^-(\tau) = \frac{t_f^5}{720}\Bigg(\pi_1\Big(\tau_1^4(15\tau^4 - 30\tau^3) + \tau_1^3(80\tau^3 - 30\tau^4) - 60\tau^3\tau_1^2 + 30\tau^4\tau_1 - 6\tau^5\Big) \\ + c_1\Big(15\tau^4 - 10\tau^3 - 6\tau^5\Big)\Bigg) + x_0 \end{aligned} \tag{C12}$$

and for times $t \geq t_1$ the expression is:

$$\begin{aligned} x^+(\tau) = \frac{t_f^5}{720}\Bigg(\pi_1\Big(\tau_1^4(15\tau^4 - 30\tau^3 + 30\tau - 15) + \tau_1^3(-30\tau^4 + 80\tau^3 - 60\tau^2 + 10)\Big) \\ + c_1\Big(-6\tau^5 + 15\tau^4 - 10\tau^3 + 1\Big)\Bigg) + x_f \\ = x^-(\tau) + \pi_1 \frac{{t_f}^5(\tau - \tau 1)^5}{120} \end{aligned} \tag{C13}$$

where c_1 and π_1 are constants, $\tau = t/t_f$ and $\tau_1 = t_1/t_f$.

The same expressions are obtained for y^+ and for y^- with π_2 and c_2 replacing π_1 and c_1 . Substituting $x^+(t_1) = x^-(t_1) = x_1$ in equations (C12) and (C13) and solving for π_1 and c_1, we obtain the following expressions :

$$c_1 = \frac{1}{t_f^5 \tau_1^2 (1-\tau_1)^5}\Big((x_f - x_0)(300\tau_1{}^5 - 1200\tau_1{}^4 + 1600\tau_1{}^3) + \tau_1{}^2(-720x_f + 120x_1 + 600x_0) + (x_0 - x_1)(300\tau_1 - 200)\Big) \qquad (C14)$$

$$\pi_1 = \frac{1}{t_f{}^5 \tau_1{}^5 (1-\tau_1)^5}\Big((x_f - x_0)(120\tau_1{}^5 - 300\tau_1{}^4 + 200\tau_1{}^3) - 20(x_1 - x_0)\Big) \qquad (C15)$$

and for π_2 and c_2 similarly, with y_0 replacing x_0 and y_f replacing x_f etc .

Next ,we substitute the expressions for π_1, π_2, c_1 and c_2 in equation (C10) which reduces to

$$\pi_1 u(t_1) + \pi_2 v(t_1) = 0 \qquad (C16)$$

and we get a polynomial equation in $\tau_1 = t_1/t_f$. We find the real roots of this polynomial and accept only those roots that lie between 0 and 1. The polynomials we obtained had only one acceptable root. We then substitute this value for τ_1 in the expressions for π_1, π_2, c_1 and c_2 and we can finally get the expressions for x(t) and y(t) for the entire movement.